Experimental observation of the trapped particle pinch effect

John Kline,[1] Scott Robertson,[2] Matt Triplett,[2] and Bob Walch[3]
[1]*Department of Physics, West Virginia University, Morgantown, West Virginia 26506*
[2]*Department of Physics, University of Colorado, Boulder, Colorado 80309-0390*
[3]*Department of Physics, University of Northern Colorado, Greeley, Colorado 80639*
(Received 22 November 2000; published 19 April 2001)

The trapped particle pinch effect (Ware's drift) has been observed in a non-neutral plasma of electrons in a modified Malmberg-Penning trap in which electrons are contained in the annular volume between concentric cylinders. A pulsed azimuthal electric field is applied by increasing the flux within a solenoid on the axis. Radial displacements of the electrons are observed which show that they remain on a surface enclosing constant axial flux. These displacements are independent of the azimuthal field and thus are consistent with Ware's drift and inconsistent with the guiding center drift alone.

DOI: 10.1103/PhysRevE.63.056406 PACS number(s): 52.27.Jt, 52.25.Fi, 52.55.Dy

I. INTRODUCTION

Transport of particles and energy in toroidal plasma devices is often dominated by particles trapped in localized minima of the magnetic field. These minima occur due to the toroidal geometry which causes the magnetic field to be smaller further from the major axis. In 1970, Ware [1] showed that these locally trapped particles do not drift in the usual way in response to the toroidal electric field used for Ohmically heating the plasma. These particles bounce back and forth along a field line and alternately gain and lose energy from the azimuthal electric field. This results in their orbits being asymmetric with respect to the midplane because the particles have more energy at one end of the bounce orbit than the other. Ware's analysis showed that the center of the bounce motion moves radially at the velocity $v_r = E_\theta / B_z$ where B_z is the axial component of the magnetic field at the midplane and E_θ is the azimuthal electric field. The guiding center drift $\mathbf{E}\times\mathbf{B}/B^2$ gives a different value of the radial drift speed $E_\theta B_z / B^2$. For the tokamak, $B_\theta \gg B_z$ and the guiding center drift formula gives a drift speed of approximately $E_\theta B_z / B_\theta^2$ that is much smaller than the true drift speed. The guiding centers drift at the $\mathbf{E}\times\mathbf{B}/B^2$ rate, but there are additional contributions to the radial drift speed from the unequal drifts at the orbit tips. Careful measurements of tokamak transport often show a radially inward flux [2], but clear identification of Ware's drift has been difficult due to the many transport processes that occur simultaneously. Ware's drift may be expressed as a mobility, $\mu_{r,\theta} = v_r / E_\theta = B_z^{-1}$, and in this form it is a transport coefficient in the neoclassical theory [3,4].

Our experiments are performed in a device [5–7] Fig. 1, which has the conditions for observation of the drift: axisymmetry and locally trapped particles that are not free to encircle the major axis. The device is similar to the cylindrical Malmberg-Penning trap in which electrons are confined radially by an axial magnetic field and confined axially by negatively biased electrodes at the ends [8,9]. Ware [1] pointed out that the increased drift rate would also apply to electrostatically trapped particles. The azimuthal magnetic field makes Ware's drift different from the guiding center drift so that the data can be shown to be consistent with one and not the other.

In Sec. II below, Ware's drift is derived from conservation of canonical angular momentum and from motion of the guiding center. In Sec. III the apparatus is described, in Sec. IV the data are presented, and Sec. V is a summary.

II. WARE'S DRIFT

The drift caused by E_θ may easily be found from the conservation of canonical angular momentum that follows from axisymmetry. The electric field is made by a flux change in a solenoid having a radius r_s that is smaller than the particle coordinate r. The magnetic vector potential may be divided into two parts, $A_{\theta,0} = \frac{1}{2} r B_z$ which arises from the uniform confining field B_z, and $A_{\theta,s} = \frac{1}{2}(r_s^2/r) B_s$ which arises from the field B_s within the solenoid. The canonical angular momentum is

$$P_\theta = r(m v_\theta + e A_\theta) = r\{m v_\theta + \tfrac{1}{2} e[r B_z + (r_s^2/r) B_s]\}, \tag{1a}$$

where v_θ is the azimuthal electron velocity, and e and m are the electron charge and mass, respectively. This equation may be averaged over a cyclotron period to obtain

$$P_\theta = r_{\rm gc}\{m v_{\theta,{\rm gc}} + \tfrac{1}{2} e[r_{\rm gc} B_z + (r_s^2/r_{\rm gc}) B_s]\}, \tag{1b}$$

where $r_{\rm gc}$ is the guiding center coordinate and $v_{\theta,{\rm gc}}$ is the azimuthal velocity of the guiding center. This velocity consists of the azimuthal guiding center drifts (electric, inertial, and magnetic gradient) and the azimuthal component of the motion along the field line. The equation may be averaged again over a bounce period to obtain

$$P_\theta = r_{\rm doc}\{m v_{\theta,{\rm doc}} + \tfrac{1}{2} e[r_{\rm doc} B_z + (r_s^2/r_{\rm doc}) B_s]\}, \tag{1c}$$

where $r_{\rm doc}$ is the radial coordinate of the drift orbit center and $v_{\theta,{\rm doc}}$ is the azimuthal velocity of the drift orbit center which is the sum of azimuthal drifts.

The mechanical momentum $r m v_\theta$ in Eq. (1a) is much smaller than the electromagnetic part of the momentum $r e A_\theta$ since the Larmor radius is much smaller than the radial co-

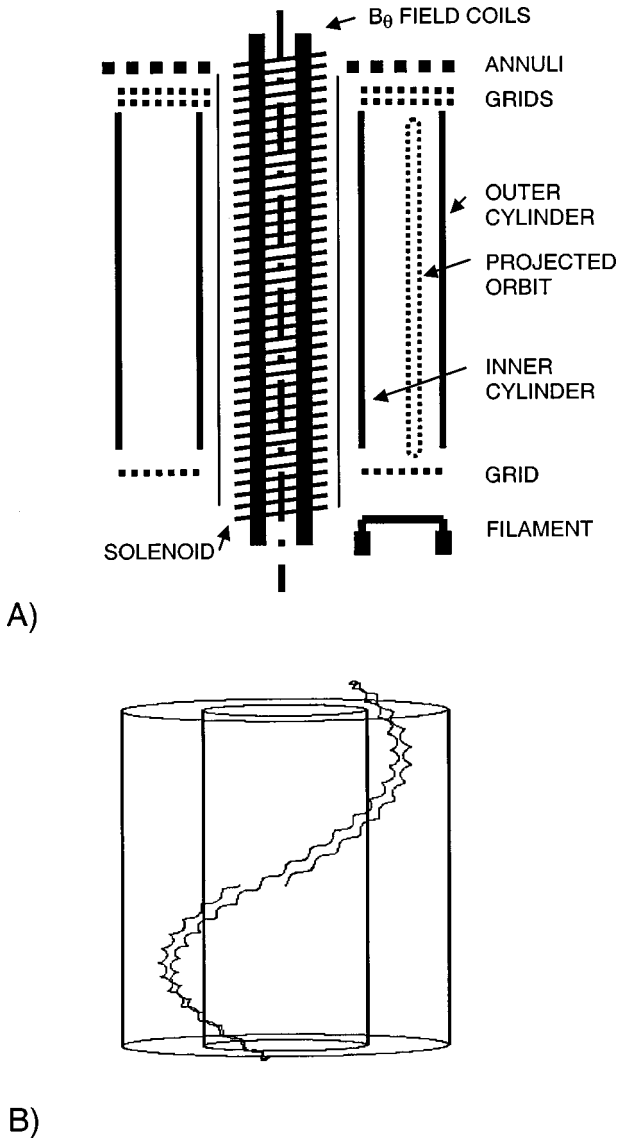

FIG. 1. (A) Schematic diagram of the annular trap. Electrons are trapped by negative potentials on the end grids. The trapped electrons are secondaries created by energetic electrons passed through the trap from the filament at one end. After being displaced by Ware's drift, the confined electrons are dumped onto the annular collectors by removing the confining potential at that end. Not shown are the Helmholtz coils for the axial field. (B) Computed orbit of an electron at low magnetic fields ($B_\theta = B_z = 2$ mT) that shows the Larmor radius and the drift orbit width. In this view the cylinders are tipped forward and the scale is approximately the same as in (A).

ordinate r. The mechanical momentum remains smaller when the equation is averaged, thus conservation of P_θ is equivalent to rA_θ remaining constant at the particle's location. For axisymmetric systems, the enclosed flux $\psi(r)$ is related to the vector potential through $A_\theta = \psi(r)/2\pi r$, thus in Eq. (1c) conservation of rA_θ requires that the drift orbit center remain on a surface enclosing constant flux.

The azimuthal electric field from the changing flux is

$$E_\theta = -(d\psi_s/dt)/2\pi r = -\tfrac{1}{2}(r_s^2/r)(dB_s/dt), \qquad (2)$$

where $\psi_s = \pi r_s^2 B_s$ is the flux from the current in the solenoid. Conservation of rA_θ requires, from Eq. (1c),

$$r_{\rm doc}(dr_{\rm doc}/dt)B_z = -\tfrac{1}{2}r_s^2(dB_s/dt) = r_{\rm doc}E_\theta, \qquad (3)$$

which implies that $dr_{\rm doc}/dt = E_\theta/B_z$ which is Ware's drift velocity. This velocity varies inversely with the radius because the loop voltage $2\pi r E_\theta$ is independent of radius. The drift displacement may be found from conservation of enclosed flux

$$r_f^2 = r_i^2 - \Delta\psi/\pi B_z, \qquad (4)$$

where r_f is the final radius of the orbit center, r_i is the initial radius and $\Delta\psi$ is the flux change. Equation (3) may be found from Eq. (4) by taking a time derivative and using Faraday's law. In the experiment, both the drift and the displacement are observed, however, only the displacement is measured quantitatively.

The radial component of the $\mathbf{E}\times\mathbf{B}$ drift is outward at one end of the device and inward at the other thus giving the drift orbit a finite radial width when projected onto the *r,z* plane [Fig. 1(A)]. This radial width may be found from a detailed consideration of guiding center drifts. The momentum parallel to the field line, $mv_\parallel$, is reversed at the tip of the drift orbit by the time integral of the force from the confining electric field:

$$-2mv_\parallel = \int q(E_z B_z/B)dt, \qquad (5)$$

where the integral is taken from the midplane to the orbit tip and back to the midplane. The force qE_z results in a radial guiding center drift and the time integral of this drift gives the radial drift displacement responsible for the full width of the drift orbit r_d,

$$r_d = \int (E_z B_\theta/B^2)dt = 2\, m\, v_\parallel B_\theta/qBB_z. \qquad (6)$$

This drift orbit width may also be obtained from Eq. (1b) by noting that the azimuthal part of the guiding center motion along the field line, $v_\parallel B_\theta/B$, changes sign at the orbit tips and thus implies a change in $r_{\rm gc}$. Equations (1b) and (6) also correctly give the width of the drift orbit in the tokamak when B_z is interpreted as the poloidal field at the midplane.

Ware's drift may also be found from a detailed consideration of guiding center drifts. The sign of $v_\parallel$ is different at the two ends of the drift orbit thus the radial displacement in Eq. (6) is outward at one end and inward at the other. The acceleration of the electrons by E_θ results in the magnitude of $v_\parallel$ being greater at one of the two orbit tips. This up-down asymmetry results in drift orbits that do not close and repetitions of the unclosed orbit leads to drift of the orbit center. The increase in $mv_\parallel$ caused by E_θ during one of the two legs of the drift orbit is $2q(E_\theta B_\theta/B)\tau_{1/2}$, where $\tau_{1/2}$ is the time to complete half an axial bounce. From Eq. (6), the difference in the displacements at the two orbit tips is $2(E_\theta B_\theta^2/B^2 B_z)\tau_{1/2}$ and the orbit fails to close by this amount. Repeated orbits result in an average drift rate $E_\theta B_\theta^2/B^2 B_z$.

This contribution to the orbit center drift adds to the guiding center drift and the total radial drift is

$$v_r = E_\theta B_\theta^2 / B^2 B_z + E_\theta B_z / B^2 = E_\theta / B_z , \tag{7}$$

which is Ware's drift velocity.

It is interesting to contrast the behavior of axially trapped particles with those that are free to circulate about the axis. In the betatron, the application of E_θ from a changing flux causes acceleration rather than a drift. The particles encircle the axis with a Larmor radius that encloses the changing flux. The flux within the orbit is increased with time and the axial magnetic field at the particle's location is adjusted to give a constant radius of gyration. Conservation of P_θ requires that mv_θ should change to balance the change in eA_θ. On the other hand, for particles in the annular Penning trap and for trapped particles in the tokamak, the Larmor orbit does not enclose the changing flux and the tangential velocity of gyration about field lines is fixed by conservation of the magnetic moment. Thus the change in A_θ is balanced by a change in the radial location of the guiding center. For circulating particles in the tokamak, however, the orbit encloses the changing flux and the azimuthal velocity increases which may lead to ''runaway'' electrons.

III. APPARATUS

The device, Fig. 1(A), differs from the Malmberg-Penning trap [8,9] by having an inner cylinder, open to air, containing (i) an air-core solenoid for changing the flux enclosed by the plasma, and (ii) conductors for creating an optional azimuthal magnetic field. The geometry of the experiment is cylindrical rather than toroidal which simplifies analysis. Electrons are contained in the annular region between the inner and outer cylinders. The flux surfaces are cylinders and the field lines are helices. An axial field of 0–15 mT is generated by Helmholtz coils and an azimuthal field of 0–9 mT is generated by six conductors along the axis with return conductors spaced 60° apart azimuthally. The rotational transform between ends is approximately 2π when the axial and azimuthal fields are equal [Fig. 1(B)]. The radii of the concentric cylindrical walls are 25 and 48 mm and their length is 150 mm. The loss of electrons along field lines is prevented by annular grids at the ends biased to -30 V. An electron beam of 150 eV from a filament at the end is passed through the trap to create secondary electrons by impact ionization of $\sim 2\times 10^{-7}$ Torr of background gas [10]. At this low pressure, the time scale for collisional transport is several tens of milliseconds which is much longer than the duration of the experiment ($\sim$3 ms). The electron energy distribution has been measured by the retarding potential method [11] and the tail of the distribution indicates a temperature of 2.5 eV [6].

The azimuthal electric field is made by means of a central air core solenoid with a radius of 17 mm, length of 250 mm, and with 220 turns. A capacitor discharge causes the solenoid current to rise to $\leqslant$200 A in 0.5 ms and creates a field of $\leqslant$22 mT ($\leqslant 2\times 10^{-5}$ Wb) within the solenoid. During the rise of the flux there is a loop voltage of $\leqslant$0.3 V lasting 1.5 ms which is the characteristic L/R time of the solenoid. The magnetic field made outside the solenoid at the plasma location is less than 1% of the applied field B_z. A five-turn coil placed around the outer cylinder measures the loop voltage induced by the changing flux.

The sign of the solenoid flux is usually in the direction to reduce the flux and the plasma is displaced outward, resulting in a region of zero density near the inner cylinder. The displacement is determined from the density profile measured by dumping the electrons onto a set of five concentric annular electrodes at one end. Each annulus spans 4.8 mm. As the displaced plasma boundary moves across an annulus, the charge observed on that annulus is reduced. The collected charge becomes zero when the boundary has moved past the annulus. The inner boundary of the plasma remains distinct as the plasma is displaced outward and the flux necessary to displace the plasma past any annulus is easily determined. The outer boundary is displaced inward when the sign of the flux change is reversed. This boundary becomes indistinct for displacements greater than a centimeter. Thus for positive flux change, useful data are limited to motion of the outer boundary past the two outermost annuli.

An alternate diagnostic is the current to the inner and outer cylinders occurring during the displacement. The interpretation of these signals requires careful consideration of image charges [10]. Outward displacement of electrons results in a decreased image charge on the inner cylinder. The current from this cylinder to ground is recorded and has a sign opposite to that for the collection of electrons. At the outer cylinder, there is a signal corresponding to the collection of electrons but this is reduced in magnitude by the decreasing positive image charge which flows to ground in the same wire.

IV. EXPERIMENT

In Fig. 2 are oscillograms showing operation of the experiment with $B_z = 15$ mT and $B_\theta = 0$. The filament bias potential is removed at 0.3 ms to stop the filling of the trap. At 1.4 ms, 60 V is applied to the solenoid creating a reduction in flux. During the flux change there is a loop voltage of $\sim$0.3 V that goes to zero at the peak in the discharge current. Ware's drift causes the electrons to move to greater radii, which results in currents of opposite signs being recorded at the inner and outer cylinders. Figure 2 shows the current collected at the outer cylinder for both inward and outward motion. The sign of the current reverses with reversal of the flux change. The current is smaller in magnitude for outward motion as a result of the electron collection being partially canceled by the change in the image charge. At 3.1 ms, when the loop voltage has gone to zero, the charge is dumped onto the annuli. The total charge is typically $\sim$10 pC, the volume between the cylinders is approximately 780 cm^3, thus the average density is $\sim 10^5\ cm^{-3}$.

Figure 3 is a set of histograms showing the radial distributions of charge measured by dumping the electrons onto the annuli. Distributions are measured with successively larger flux changes. The histograms show that the plasma is displaced toward greater radii when the enclosed flux is de-

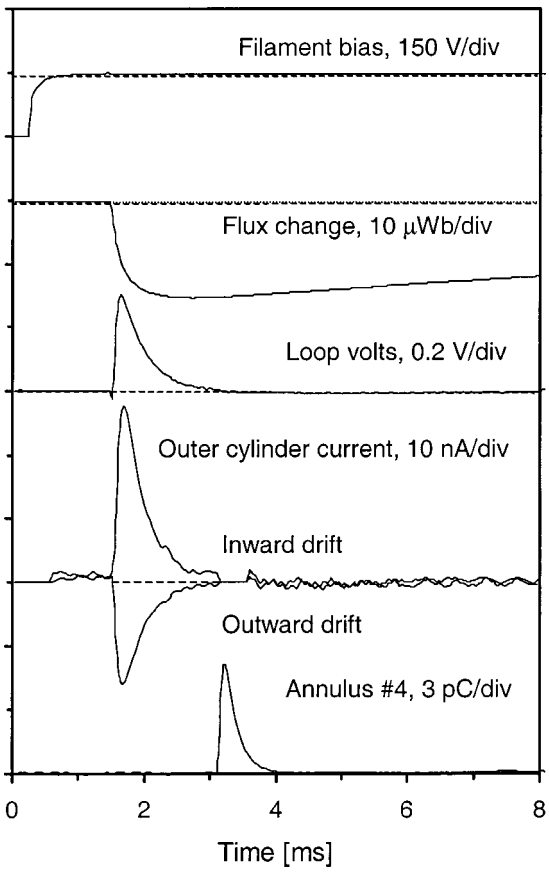

FIG. 2. Oscillograms showing operation of the experiment. The filament bias is removed at 0.3 ms and at 1.4 ms the flux is changed, creating a pulse of loop voltage during which current is recorded at the outer cylinder. This signal is reversed when the polarity of the flux change is reversed. At 3.1 ms, the charge is dumped onto five concentric annuli. The signal at the fourth annulus from the inner cylinder is shown.

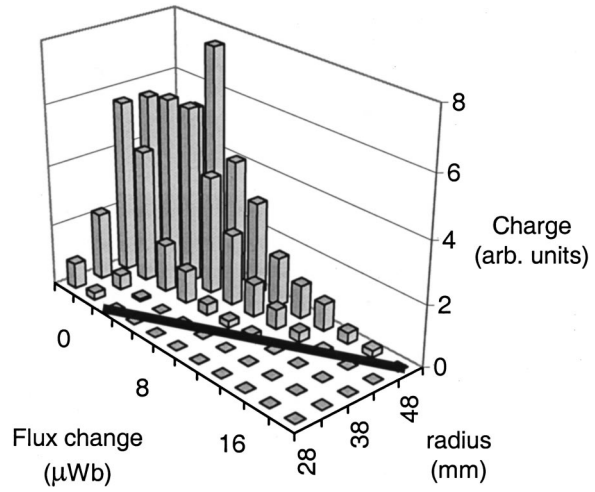

FIG. 3. Histograms of the collected charge (arbitrary units) as a function of radius and of the absolute value of the flux within the solenoid. The solid line is the displacement of the inner plasma boundary corresponding to constant enclosed flux [Eq. (4)].

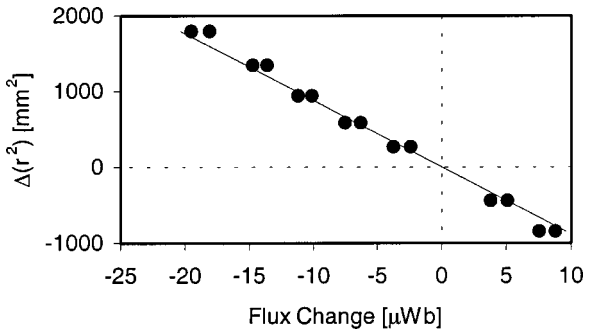

FIG. 4. Plot of the change in r^2 as a function of the flux change for $B_z=9$ mT where r is the boundary location. The close pairs of points mark the highest value at which charge is seen at the given location and the lowest value at which charge is absent. The data for negative flux change is from the outward motion of the inner boundary and the data for positive flux change is from inward motion of the outer boundary.

creased. The solid line shows the location of the inner plasma boundary calculated from Eq. (4).

Figure 4 shows the change in r_f^2 as a function of flux change for an axial field of 9 mT. The flux is increased in

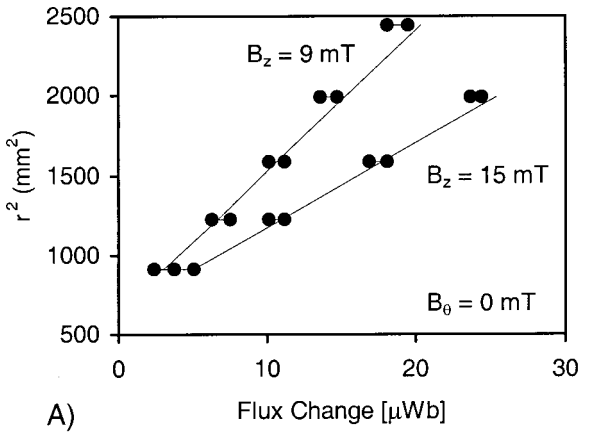

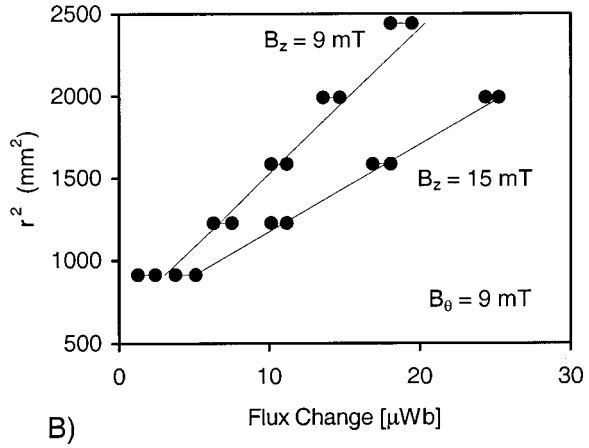

FIG. 5. (A) The square of the radius of the inner boundary as a function of the absolute value of the flux change for $B_\theta=0$ and for $B_z=9$ and 15 mT. (B) Data as in (A) with B_θ increased to 9 mT. The solid lines are from Eq. (4).

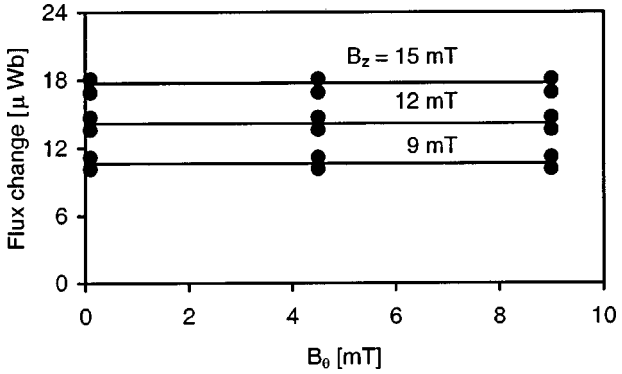

FIG. 6. Flux required for a displacement of 14.4 mm for three values of axial field (9, 12, and 15 mT) and three values of azimuthal field (0, 4.5, and 9 mT). The solid lines are the flux changes from Eq. (4).

small steps of 1.2 μWb in order to tightly bracket the value at which the plasma boundary is displaced past each annulus. The close pairs of points in the plot are the last value of flux change at which electrons were seen and the first value at which electrons were absent. For inward displacement, the location of the outer boundary is used and for outward displacement the inner boundary is used. The data show the expected linear relationship between the change in the square of the radius and the flux change [Eq. (4)]. The measured flux changes are systematically about 8% lower than the calculated flux changes in all data sets. This difference is not considered significant and may arise from an error in the calculated relationship between the flux change and the diagnostic signal for the solenoid current.

Additional data were taken at axial fields of 9, 12, and 15 mT and azimuthal fields of 0, 4, 5, and 9 mT. A subset of these data that omits (for clarity) the middle values of the fields is shown in Fig. 5. The displacement at a given flux change is smaller at the higher value of axial field because the smaller displacement encloses a larger flux. A comparison of data for $B_\theta = 0$ [Fig. 5(A)] with that for $B_\theta = 9$ mT [Fig. 5(B)] shows that the azimuthal field has negligible effect on the displacement. This point is illustrated more clearly in Fig. 6 which shows the flux change required to displace the boundary the width of three annuli (14.4 mm). This figure includes points from all nine data sets and the solid lines are the flux changes calculated from Eq. (4). The flux changes have the expected linear dependence upon the axial field B_z and are independent of the azimuthal field B_θ. If the drift distance were determined by the guiding center drift formula rather than Ware's drift, the required flux at $B_z = 9$ mT would have increased a factor of 2 as B_θ was increased from 0 to 9 mT.

V. SUMMARY

An annular version of the Malmberg-Penning trap has been used to investigate the particle drifts arising from an azimuthal electric field created by a changing flux in a solenoid on the cylindrical axis. Conservation of canonical angular momentum requires that the electrons remain on a flux surface. This requires that the bounce-averaged particle locations (the drift orbit centers) should move radially at Ware's drift velocity rather than at the slower guiding center drift velocity. The application of an azimuthal magnetic field allows the guiding center drift $E_\theta B_z / B^2$ to be distinguished from Ware's drift E_θ / B_z. The drift distance is determined experimentally by dumping the electrons onto a set of five concentric annuli. Comparison of data sets taken over a wide range of B_z and B_θ shows that the drift distances are very nearly that determined by Ware's drift and are significantly different from that determined by the guiding center drift alone.

ACKNOWLEDGMENTS

The authors acknowledge valuable discussions with John Cary, Scott Parker, Qudsia Quraishi, and Earl Scime.

[1] A. A. Ware, Phys. Rev. Lett. **25**, 15 (1970).
[2] See, for example, R. J. Hawryluk, in *Physics of Plasmas Close to Thermonuclear Conditions, 1979*, Proceedings of the Course of the International School of Plasma Physics (Commission of the European Communities, Brussels, 1980), Vol. 1, p. 19.
[3] B. B. Kadomtsev and O. P. Pogutse, Nucl. Fusion **11**, 67 (1971).
[4] F. L. Hinton and R. D. Hazeltine, Rev. Mod. Phys. **48**, 239 (1976).
[5] S. Robertson and B. Walch, Rev. Sci. Instrum. **70**, 2993 (1999).
[6] J. Kline, S. Robertson and B. Walch, in *Non-Neutral Plasma Physics III*, edited by J. J. Bollinger, R. L. Spencer, and R. C. Davidson, AIP Conf. Proc. No. 498 (AIP, New York, 1999), p. 290.
[7] Q. Quraishi and S. Robertson, Phys. Rev. E **62**, 1405 (2000).
[8] J. H. Malmberg, C. F. Driscoll, B. Beck, D. L. Eggleston, J. Fajans, K. Fine, X.-P. Huang, and A. W. Hyatt, in *Non-Neutral Plasma Physics*, edited by C. W. Roberson and C. F. Driscoll, AIP Conf. Proc. No. 175 (AIP, New York, 1988), p. 28.
[9] D. L. Eggleston, Phys. Plasmas **4**, 1196 (1997).
[10] B. Walch and S. Robertson, Phys. Plasmas **7**, 2340 (2000).
[11] D. L. Eggleston, C. F. Driscoll, B. R. Beck, A. W. Hyatt, and J. H. Malmberg, Phys. Fluids B **4**, 3432 (1992).